Prediction of Meiyu rainfall in Taiwan by multi-lead physical–empirical models

So-Young Yim, Bin Wang, Wen Xing & Mong-Ming Lu

Climate Dynamics
Observational, Theoretical and Computational Research on the Climate System

ISSN 0930-7575
Volume 44
Combined 11-12

Clim Dyn (2015) 44:3033-3042
DOI 10.1007/s00382-014-2340-0

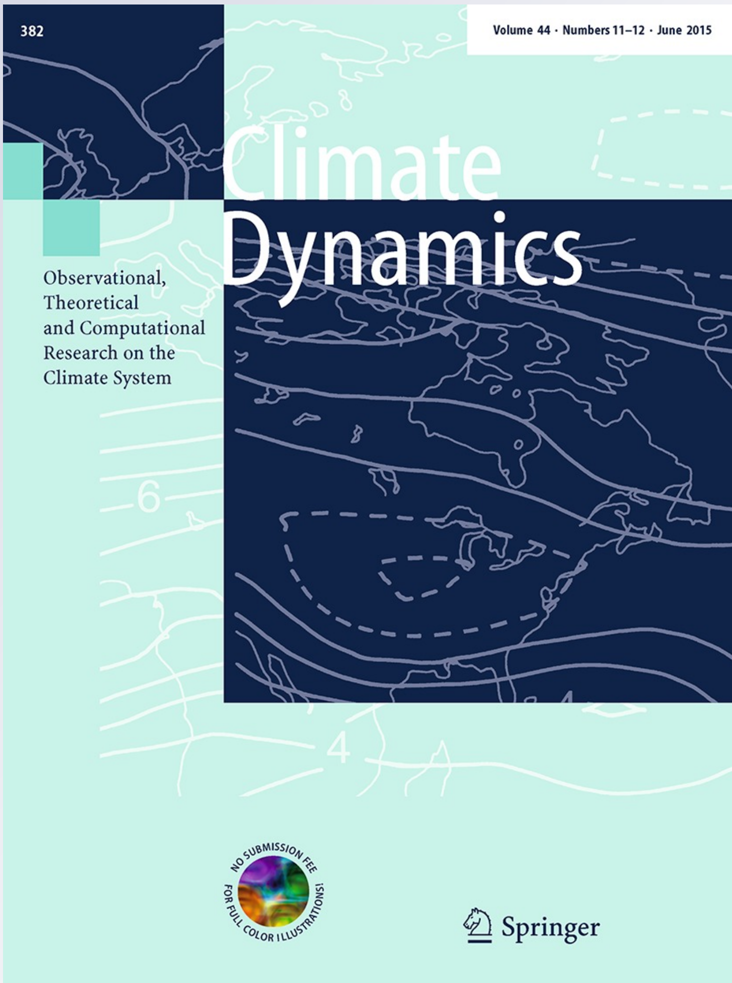

Springer

Clim Dyn (2015) 44:3033–3042
DOI 10.1007/s00382-014-2340-0

Prediction of Meiyu rainfall in Taiwan by multi-lead physical–empirical models

So-Young Yim · Bin Wang · Wen Xing · Mong-Ming Lu

Received: 27 January 2014 / Accepted: 15 September 2014 / Published online: 28 September 2014

Abstract Taiwan is located at the dividing point of the tropical and subtropical monsoons over East Asia. Taiwan has double rainy seasons, the Meiyu in May–June and the Typhoon rains in August–September. To predict the amount of Meiyu rainfall is of profound importance to disaster preparedness and water resource management. The seasonal forecast of May–June Meiyu rainfall has been a challenge to current dynamical models and the factors controlling Taiwan Meiyu variability has eluded climate scientists for decades. Here we investigate the physical processes that are possibly important for leading to significant fluctuation of the Taiwan Meiyu rainfall. Based on this understanding, we develop a physical–empirical model to predict Taiwan Meiyu rainfall at a lead time of 0- (end of April), 1-, and 2-month, respectively. Three physically consequential and complementary predictors are used: (1) a contrasting sea surface temperature (SST) tendency in the Indo-Pacific warm pool, (2) the tripolar SST tendency in North Atlantic that is associated with North Atlantic Oscillation, and (3) a surface warming tendency in northeast Asia. These precursors foreshadow an enhanced Philippine Sea anticyclonic anomalies and the anomalous cyclone near the southeastern China in the ensuing summer, which together favor increasing Taiwan Meiyu rainfall. Note that the identified precursors at various lead-times represent essentially the same physical processes, suggesting the robustness of the predictors. The physical empirical model made by these predictors is capable of capturing the Taiwan rainfall variability with a significant cross-validated temporal correlation coefficient skill of 0.75, 0.64, and 0.61 for 1979–2012 at the 0-, 1-, and 2-month lead time, respectively. The physical–empirical model concept used here can be extended to summer monsoon rainfall prediction over the Southeast Asia and other regions.

Keywords Physical–empirical model · Seasonal forecast · Meiyu rainfall · East Asian summer monsoon · Philippine Sea anticyclone · North Atlantic Oscillation

1 Introduction

Taiwan is a mid-size island located at the western boundary of the subtropical Pacific with the Tropic of Cancer running across. Even though the area of Taiwan is only about 36,000 square kilometers, there are six mountain peaks over 3,500 m and the highest peak Yushan is at 3,952 m. The integrated monsoonal and terrain effects result in a unique rainfall pattern in Taiwan. Taiwan's climate variability is influenced by East Asian and western North Pacific monsoons (e.g., Boyle and Chen 1987; Tao and Chen 1987; Chen et al. 2010) and complicated by the topographic effects (e.g., Chen et al. 1999; Yen and Chen 2000) and abundant moisture supply from the surrounding ocean.

S.-Y. Yim
Korea Meteorological Administration, Seoul 156-720, Korea

B. Wang · W. Xing
International Pacific Research Center and Department of Atmospheric Sciences, University of Hawaii at Manoa, Honolulu, HI 96822, USA

B. Wang
Earth System Modeling Center, Nanjing University of Information Science and Technology, Nanjing 210044, China

M.-M. Lu (✉)
Research and Development Center, Central Weather Bureau, Taipei 10048, Taiwan
e-mail: lu@rdc.cwb.gov.tw

Fig. 1 Pentad climatology of rainfall amount averaged over Taichung station for the period 1911–2010

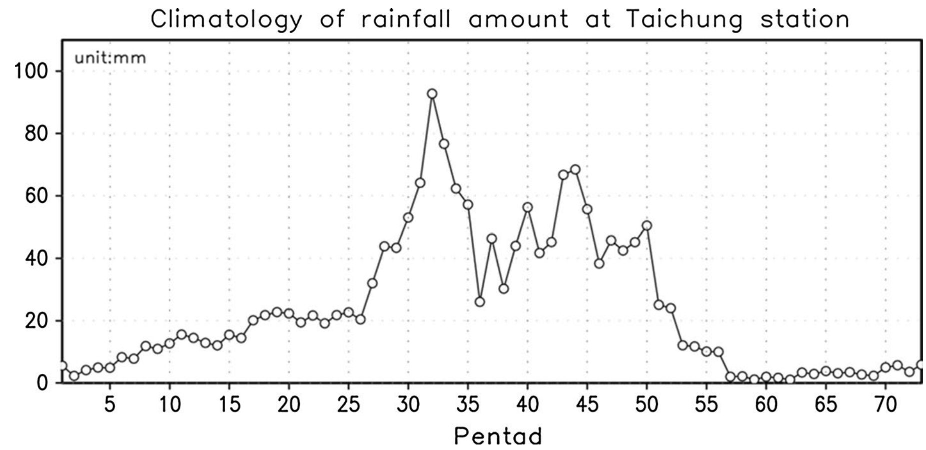

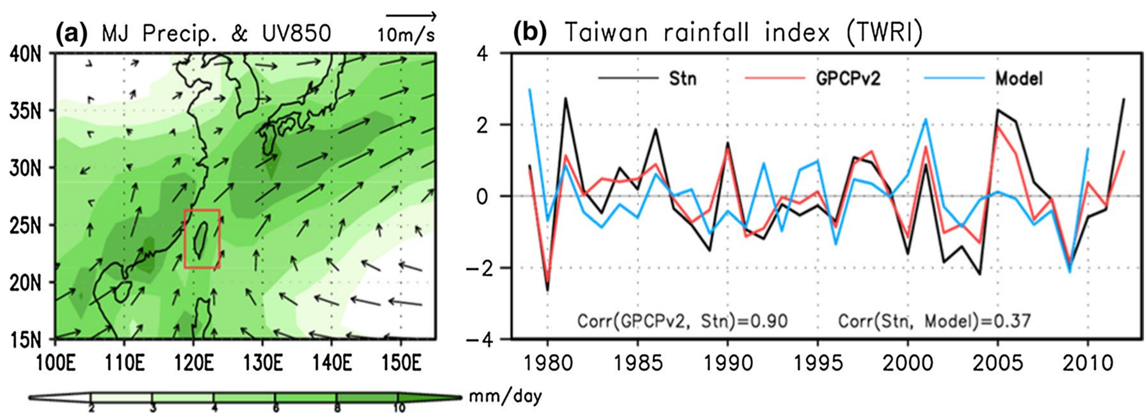

Fig. 2 **a** Climatological May–June (MJ) mean precipitation (mm/day) and 850-hPa winds (m/s). **b** The normalized time series of MJ rainfall anomaly averaged over Taiwan region for the period 1979–2012. For comparison, the Taiwan rainfall index (TWRI) derived from the 24 stations data (*black*), and the multi-model retrospective prediction of the TWRI (*blue*) are also plotted in (**b**). The *red box* in (**a**) indicates the Taiwan region (119E–123E, 21N–26N) when GPCP data (*red*) are used to make an area averaged TWRI. The four coupled models' ensemble mean initiated from the first day of May for the 32 years of 1979–2010 are used

The pentad climatology based on 100 years (1911–2010) rainfall data at Taichung station located at the central part of the island near the west coast (Fig. 1) shows a sharp peak at pentad 32 (June 5–9). The accumulated rainfall amount during the 10 pentads from pentad 27 (May 11–15) to 36 (June 25–20) makes up about one third of the annual total. This distinct rainy period is called Meiyu season in Taiwan (Chen 1983; Wang et al. 1984). The climatological precipitation during Meiyu season shows a large-scale spatial structure: a rain band oriented in the southwest-northeast direction near Taiwan is clearly observed (Fig. 2a). The centers of rainfall maximum appear over northern Vietnam (19N, 104E), South China coast (22N, 114E), Taiwan (24N, 120E), and south of Japan. After the Meiyu season, there is a dry period in early July followed by another peak in August–September due to typhoon rainfall (Fig. 3 in Wang and LinHo 2002; Chen et al. 2007, 2010). The present study focuses on the variability of Taiwan Meiyu during May–June (MJ) season.

Meiyu is the first intensive rainy period after the dry season from October to April. To predict the onset and duration of the Meiyu as well as the amount of rainfall and its intensity is of profound importance to disaster preparedness and water resource management. Although the average annual total rainfall amount averaged over Taiwan is about 2,500 mm, the rainfall per capita per year is about 3,913 m^3 that is 12 % of the world average. Taiwan actually ranks the 18th on the world list of water-scarce countries. Therefore, the demand for rainfall prediction information from sub-seasonal to seasonal scales is extremely high. In addition, the seasonal precipitation prediction skill is poor in East Asia (Wang et al. 2009a). As shown in Fig. 2b, the temporal correlation coefficient between observed and the forecasted precipitation by the 4 state-of-the-art multi-model ensemble mean in the rectangular region around Taiwan (119E–123E and 21N–26N) is only 0.37. It suggests more study is needed to meet the high demand of forecast information of Meiyu seasonal rainfall in Taiwan area.

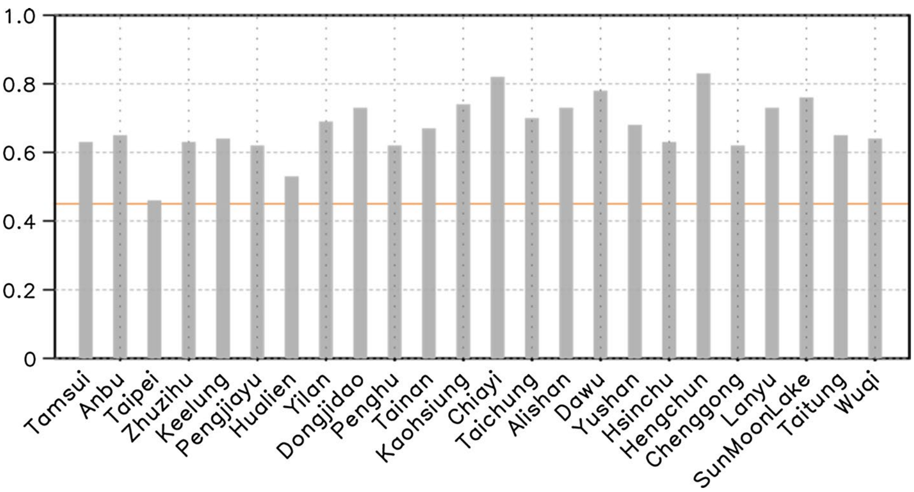

Fig. 3 Correlation coefficients between the rain gauge at 24 Taiwan stations and GPCP-TWRI. All correlation coefficients are statistically significant at 99 % confidence level

The objectives of this study are to understand the sources of interannual variability and predictability of the seasonal rainfall amount in Taiwan during the Meiyu season (MJ), and to establish a physics-based empirical (PE) prediction model. The prediction skill of the prediction model will be evaluated following the standard procedure of seasonal forecast recommended by WMO Lead Center for Standard Verification System of Long Range Forecasts (LC-SVS-LRF, http://www.bom.gov.au/wmo/lrfvs/users.shtml). The practical prediction skill also provides an estimate of the practical predictability of the Taiwan Meiyu.

2 Data and methodology

The precipitation data used are derived from 24 conventional stations in Taiwan for the period 1979–2012 administrated by the Central Weather Bureau (CWB) (Fig. 1 in Chen et al. 2004). For comparison, Global Precipitation Climatology Project (GPCP) version 2.2 dataset (Huffman et al. 2011) are also used. To measure Taiwan Meiyu variation, May–June precipitation is averaged over the region near Taiwan (119E–123E, 21N–26N). For simplicity it is called GPCP Taiwan Meiyu rainfall index (GPCP-TWRI). The precipitation rates at all 24 stations are significantly correlated with the GPCP-TWRI over the 99 % confidence level and their correlation coefficients range from 0.60 to 0.82 except two stations (Fig. 3). As a result, all Taiwan Meiyu rainfall averaged over the 24 stations (StnTWRI) during MJ season shows a good agreement ($r = 0.90$) with the GPCP TWRI as shown in Fig. 2b.

The atmospheric circulation and sea surface temperature (SST) data were obtained from the newly released ERA interim (Dee et al. 2011) and the National Oceanic and Atmospheric Administration extended reconstructed SST (ERSST) version 3 (Smith et al. 2008), respectively.

Stepwise regression was used to establish the prediction equations. Prior to regression, all variables are normalized by removing their means and divided by their corresponding standard deviation, which allows a direct comparison of the relative contribution of each predictor by examining the normalized regression coefficient. The stepwise procedure helps selecting statistically important predictors at each step. The significance of each predictor selected is based on its significance in increasing the regressed variance by a standard F test (Panofsky and Brier 1968). A 95 % statistical significance level is used as a criterion to select new predictor at each step. Once selected into the model, a predictor can only be removed if its significance level falls below 95 % by the addition/removal of another variable. To avoid over-fitting, we require the number of selected predictors is less than 10 % of the sample size.

The product of multi-model ensemble forecast system is used as a reference for evaluating the prediction skill of the physical–empirical prediction model developed in this study. The 4 state-of-the-art atmosphere–ocean–land coupled models used are NCEP CFS version 2 (Saha et al. 2014), ABOM POAMA version 2.4 (Hudson et al. 2011), GFDL CM version 2.1 (Delworth et al. 2006), and FRCGC SINTEX-F model (Luo et al. 2005), which were adopted from Asia–Pacific economic cooperation climate center (APCC)/climate prediction and its application to society (CliPAS).

3 Precipitation and circulation anomalies associated with a strong Meiyu over Taiwan

The MJ precipitation anomalies in Taiwan area have significant interannual variability (Fig. 2b). To see what large-scale circulation anomalies affect Taiwan Meiyu, the correlation maps of the precipitation and 850-hPa

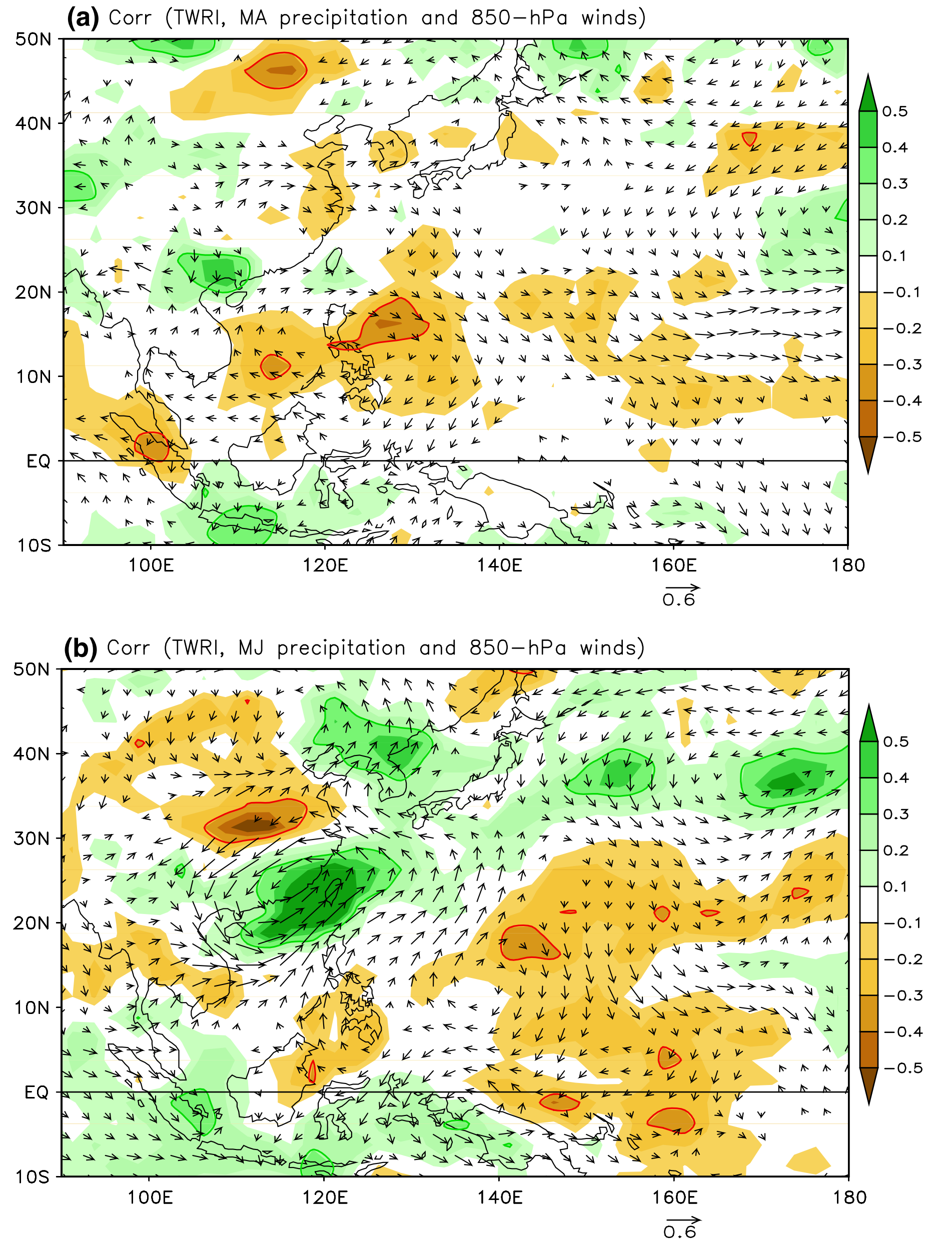

Fig. 4 Correlation maps of precipitation (*shading*) and 850 hPa wind anomalies (*vector*) during **a** March–April and **b** May–June with respect to the time series of GPCP-TWRI. The *contours* show a 90 % significant confidence for precipitation

wind anomalies with reference to Taiwan Meiyu rainfall (GPCP-TWRI) are depicted in Fig. 4 for March–April and MJ. Prior to a strong Taiwan Meiyu in March–April, an enhanced precipitation associated with southerly wind anomalies is seen in southeastern China. The South China Sea is under control of the western North Pacific subtropical high (WNPSH) and experiences a dry weather regime (Fig. 4a). During May–June, the WNPSH retreats from South China Sea eastward to the Philippine Sea (Fig. 4b). Meanwhile a strong anomalous cyclonic circulation firmly controls southeast China with enhanced southwesterlies in between the cyclone and WNPSH, leading to enhanced rainfall centered on Taiwan and reduced rainfall over the central eastern China. In sum, a strong Taiwan Meiyu is associated with building up of the pressure gradients between southeast China low and Philippine Sea subtropical high and associated southwesterly monsoon flows.

4 Physical consideration on the Taiwan Meiyu predictors

There are two circulation systems that are important to enhanced Taiwan Meiyu: the enhanced anticyclonic circulation over the Philippine Sea and the cyclonic anomaly over the southeast coast of China (Fig. 4).

The Philippine Sea anomalous anticyclone that is excited during winter time can maintain itself until early summer through a positive thermodynamic feedback between the Philippine Sea anticyclone and the SST dipole associated with this anticyclone in the WNP (Wang et al. 2000; Lau and Nath 2003) or over the Indo-Pacific warm pool (Wang et al. 2013). Thus, the local SST anomaly patterns that are indicative of the local Philippine Sea anticyclone-ocean mixed layer interaction can be good candidate predictors.

The previous study found that MJ rainfall over East Asia is preceded by eastern China surface warming and low pressure anomaly (Wang et al. 2009b). This eastern China surface warming can often traced back to an even larger scale warming to the north of 40N in late winter and early spring. It has been shown that the reduced spring snow cover over Eurasia leads to surface warming over North and East Asia and signifies an increased summer precipitation in the southeast coast of China (Figs. 7 and 8 in Yim et al. 2010). Hence, the northeast Asian continental warming during the previous winter and early spring could be another type of signals to search for.

In addition, previous studies have found that the North Atlantic Oscillation (NAO) can affect EA summer monsoon (EASM) through a number of possible pathways. One is through excitation of midlatitude Eurasian wave trains to affect northeast Asian circulation and consequently the EA subtropical frontal rainfall (Wu et al. 2009; Yim et al. 2013). The second possible pathway is through its linkage to Arctic Oscillation that can change EA westerly jet stream and thus the strength of the WNPSH (Gong et al. 2011). The third pathway is through the equatorial central Pacific. The tropical Atlantic rainfall anomalies associated the NAO can excite westward propagating Rossby waves to affect eastern Pacific trade winds thus generating SST anomalies over the equatorial central Pacific, which in turn impact the strength of the Philippine Sea subtropical high (Wang et al. 2013). It was also found that the North Atlantic SST anomalies can have a positive feedback with the winds associated with the NAO, which maintains themselves from winter into MJ (Wu et al. 2009). Therefore, the SST anomalies during winter and early spring over the North Atlantic can be a potential predictor.

5 A hierarchal physical–empirical (PE) prediction models for MJ Taiwan precipitation

The selection of predictors in this study is primarily based on the physical consideration discussed in Sect. 4 and our understanding of the lead-lag linkage between the predictand and predictors. Statistical tests and stepwise regression are used as auxiliary tools to verify the statistical significance and relative independence of the selected predictors. In selection of predictors we consider SST and 2 m air temperature (T2M) representing the lower boundary anomalous conditions over the ocean and land surfaces. No circulation anomalies are selected because the seasonal circulation anomalies are driven by the interaction with the lower boundary anomalies and have little memory by themselves except the sea level pressure.

In this section, we first identified physical consequential predictors at various lead time ranging from 0- to 2-month and then establish a hierarchal physical–empirical (PE) prediction models for Taiwan MJ (Meiyu) seasonal rainfall forecast. In order to test the predictive capability of the empirical model, the cross-validation method is performed using taking out 3 years around a forecast target year. To confirm whether the suggested methodology is actually useful, we used 1979–2005 data as training period to derive prediction equations, and then made independent forecasts for the period 2006–2012 in various lead forecasts.

5.1 Zero-month lead prediction

The 0-month lead forecast model uses predictors that involve information before and during April. Based on the discussion in Sect. 4, three physical predictors are identified from the tendency field defined by March–April (MA) minus January–February (JF). The first predictor is a negative SST tendency over western North Pacific (WNPT) for a strong Taiwan Meiyu (Fig. 5a). This cooling tendency leads to enhanced westerlies north of the subtropical high over the Philippine Sea which signifies enhancement of the Philippine Sea subtropical high in March–April and lasts until MJ. This is a characteristic of a strong Meiyu over Taiwan. The second predictor is the meridional tripolar SST tendency across North Atlantic (NAT). This tripolar tendency consists of a warming process in the tropical and mid-latitude North Atlantic and a cooling in the subtropics. The NAT predictor reflects the remote impacts from North Atlantic on Taiwan Meiyu rainfall. The third predictor is the warming tendency over northeastern East Asia (EAT) across winter to early summer, which signifies a stronger Taiwan Meiyu (Fig. 5a). This warming corresponds to the decreasing tendency of SLP and the southwest extension of the decreasing SLP and warming from northeast East Asia presages the development of anomalous cyclone in MJ over the southern China.

The regions where the three predictors are defined are shown in Fig. 5a and explained in Table 1. Their correlation coefficients with the TWRI and among the predictors are summarized in Table 2. Due to their relative independence, all three predictors are selected by stepwise regression given the F–test at 95 % confidence level. The 0-month lead prediction equation is

$$\mathrm{TWRI} = -0.531 * \mathrm{WNPT} + 0.499 * \mathrm{NAT} + 0.291 * \mathrm{EAT} \quad (1)$$

Figure 6a shows the cross-validated temporal correlation skill (TCC) for the prediction using Eq. (1). The

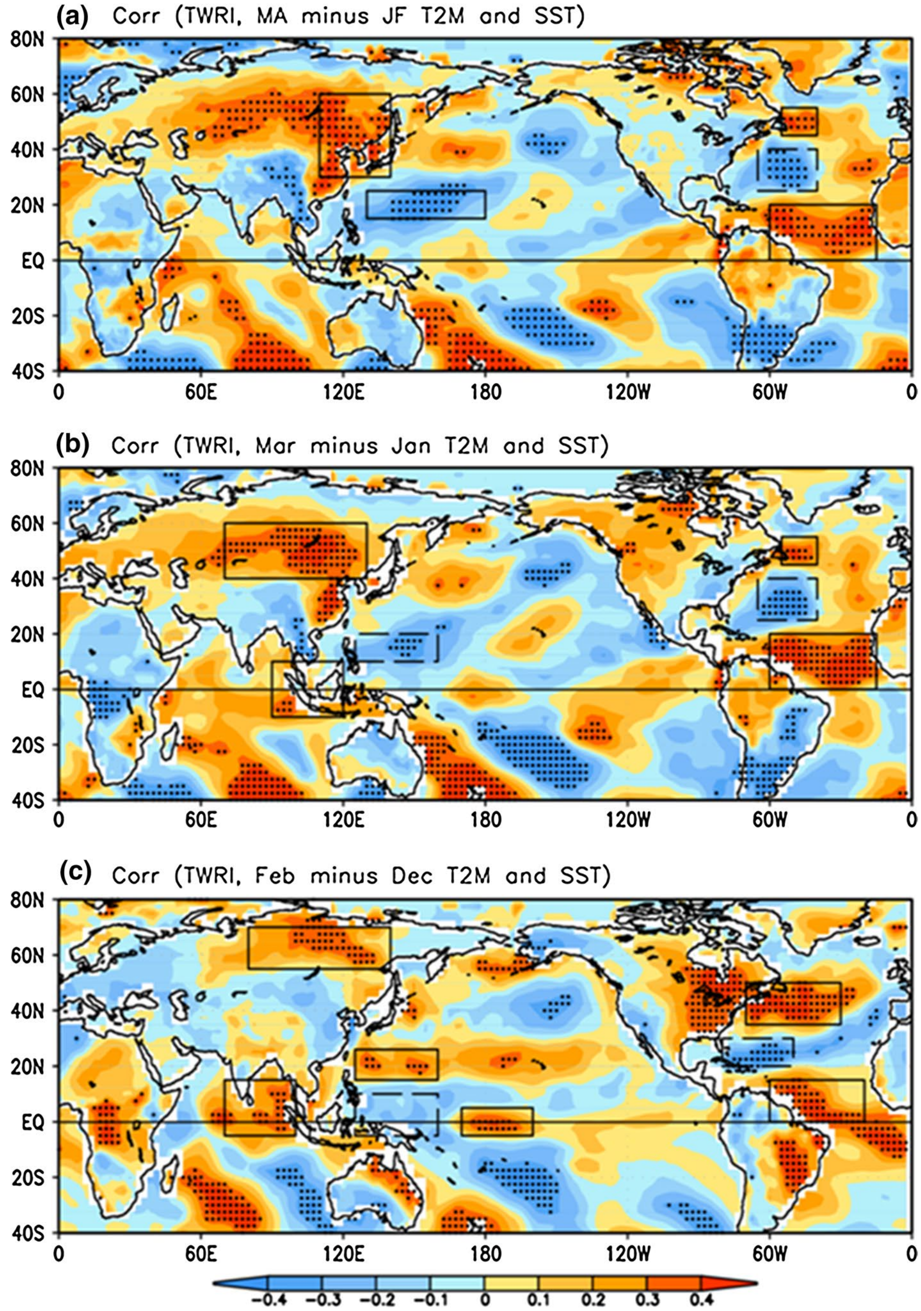

Fig. 5 Three precursors associated with MJ TWRI at 0-, 1-, and 2-month lead: Correlation coefficient of **a** MA minus JF, **b** Mar minus Jan, and **c** Feb minus Dec T2M (over land) and SST (over ocean) with respect to the time series of MJ GPCP-TWRI. The *boxes* indicate the areas where the area-averaged variables are selected for the predictors. The areas exceeding 95 % confidence level are *dotted*

physical–empirical model can reproduce the MJ Taiwan rainfall realistically with a TCC skill of 0.80 for all 34 years. The TCC for the 34 year cross-validated reforecast skill is 0.75 and the independent forecast skill for 2006–2012 is 0.81 when a prediction equation is built using the 1979–2005 data as training period.

5.2 One-month lead prediction

The 1-month lead forecast model uses predictors from March or before-March conditions. Three physical predictors are found from the tendency field defined by March minus January. The three predictors identified have similar physical meaning as the predictors used at 0-month lead forecast with slight modifications in their domain of definition. The WNPT predictor at 0-month lead is slightly modified to the IOWPT for the 1-month lead forecast. The EAT domain used in 0-month lead is also modified (a westward shift) (Fig. 5b). The IOWPT represents a dipolar SST tendency over the Indian Ocean and WNP, i.e., a warming tendency in eastern Indian Ocean and a negative SST anomaly over the Philippine Sea (Fig. 5b). Their precise definitions are presented in Table 1 and their correlation coefficients with the TWRI and among the predictors are summarized in Table 3.

Table 1 Definition of each of 0-, 1-, and 2-month lead predictors selected for the prediction of MJ Taiwan precipitation variability

Predictor	Meaning	Definition		
		0-month lead (MA-minus-JF)	1-month lead (Mar-minus-Jan)	2-month lead (Feb-minus-Dec)
WNPT	Western North Pacific SST tendency	15N–25N, 130E–180E	–	–
IOWPT	Indo-Pacific warm pool SST tendency	–	(10S–10N, 80E–120E) – (10N–20N, 125E–160E)	(5S–15N, 70E–100E) + (15N–25N, 125E–160E) + (5S–5N, 170E–160W) – (5S–10N, 125E–160E)
NAT	Tripolar North Atlantic SST tendency	(0–20N, 60W–15W) + (45N–55N, 55W–40W) – (25N–40N, 65W–40W)	(0–20N, 60W–15W) + (45N–55N, 55W–40W) – (25N–40N, 65W–40W)	(0–15N, 60W–20W) + (35N–50N, 70W–30W) – (20N–30N, 80W–50W)
EAT	East Asia T2M tendency	30N–60N, 110E–140E	40N–60N, 70E–130E	55N–75N, 90E–140E

An empirical prediction with those three predictors is made using the multiple stepwise regression method. All three predictors are selected by the stepwise regression given the F–test at 95 % confidence level. The 1-month lead prediction equation is

$$\mathrm{TWRI} = 0.393 * \mathrm{IOWPT} + 0.374 * \mathrm{NAT} + 0.329 * \mathrm{EAT} \qquad (2)$$

Figure 6b shows the validated temporal correlation skill (TCC) for the prediction using Eq. (2). The physical–empirical model is capable of capturing the MJ Taiwan rainfall with a TCC skill of 0.72 for all 34 years. The TCC for the 34 year cross-validated reforecast skill is 0.64 and the independent forecast skill is 0.52 when the prediction equation is built using the 1979–2005 data as training period.

5.3 Two-month lead prediction

To predict MJ TWRI 2-month ahead, we examined lower boundary climate anomalies in the preceding winter. Figure 5c shows the correlation map revealing the tendency fields across winter season from December to February associated with MJ TWRI. Again, the three predictors identified are consistent with the discussion in Sect. 4 and have similar physical meanings as the predictors used at 0- and 1-month lead forecasts. Slight modifications in the domains of definition are made as the seasonal mean state and anomalies evolve with season. The defintions of the winter predictors are presented in Fig. 5c and in Table 1 and their correlation coefficients with the TWRI and among the predictors are summarized in Table 4.

First, the SST tendency pattern over Indian Ocean-warm pool (IOWPT) is associated with the enhanced Taiwan rainfall in MJ. The warming tendency in Indian Ocean and central Pacific and the cooling tendency in the western Pacific can arguably favor establishing the anomalous high over the Philippine Sea and South China Sea in the preceding winter which can be maintained through spring to MJ by local positive feedback between the anticyclone and the underlying SST anomalies (Wang et al. 2000). Second, the tripolar SST tendency (NAT) over North Atlantic across winter (Fig. 5c) can interact with NAO with a positive feedback to sustain both the NAO and tripolar SST into MJ (Wu et al. 2009). The third predictor (EAT) denotes a winter warming over Siberia, in a region north of the warming tendency in early spring (Fig. 5c).

The 2-month lead prediction equation is

$$\mathrm{TWRI} = 0.406 * \mathrm{IOWPT} + 0.380 * \mathrm{NAT} + 0.147 * \mathrm{EAT} \qquad (3)$$

Figure 6c shows the validated TCC skill for the prediction using Eq. (3). The physical empirical model can reproduce the MJ Taiwan rainfall with a temporal correlation skill of 0.68 for all 34 years. The TCC for the 34 year cross-validated reforecast skill is 0.61 and the independent

Table 2 The correlation coefficients (CCs) with the predictand (GPCP-TWRI) and among the predictors for the period 1979–2012

	TWRI	WNPT	NAT	EAT
TWRI	1.0	**−0.50**	**0.47**	**0.46**
WNPT	–	1.0	0.15	−0.15
NAT	–	–	1.0	0.17
EAT	–	–	–	1.0

The bolded numbers represent significance at 95 % confidence level

forecast skill is 0.75 when a prediction equation is built using the 1979–2005 data as training period.

6 Summary

Taiwan has double rainy seasons, the Meiyu in May–June and the Typhoon rains in August–October (Fig. 1). Taiwan ranks the 18th on the world list of water-scarce countries due

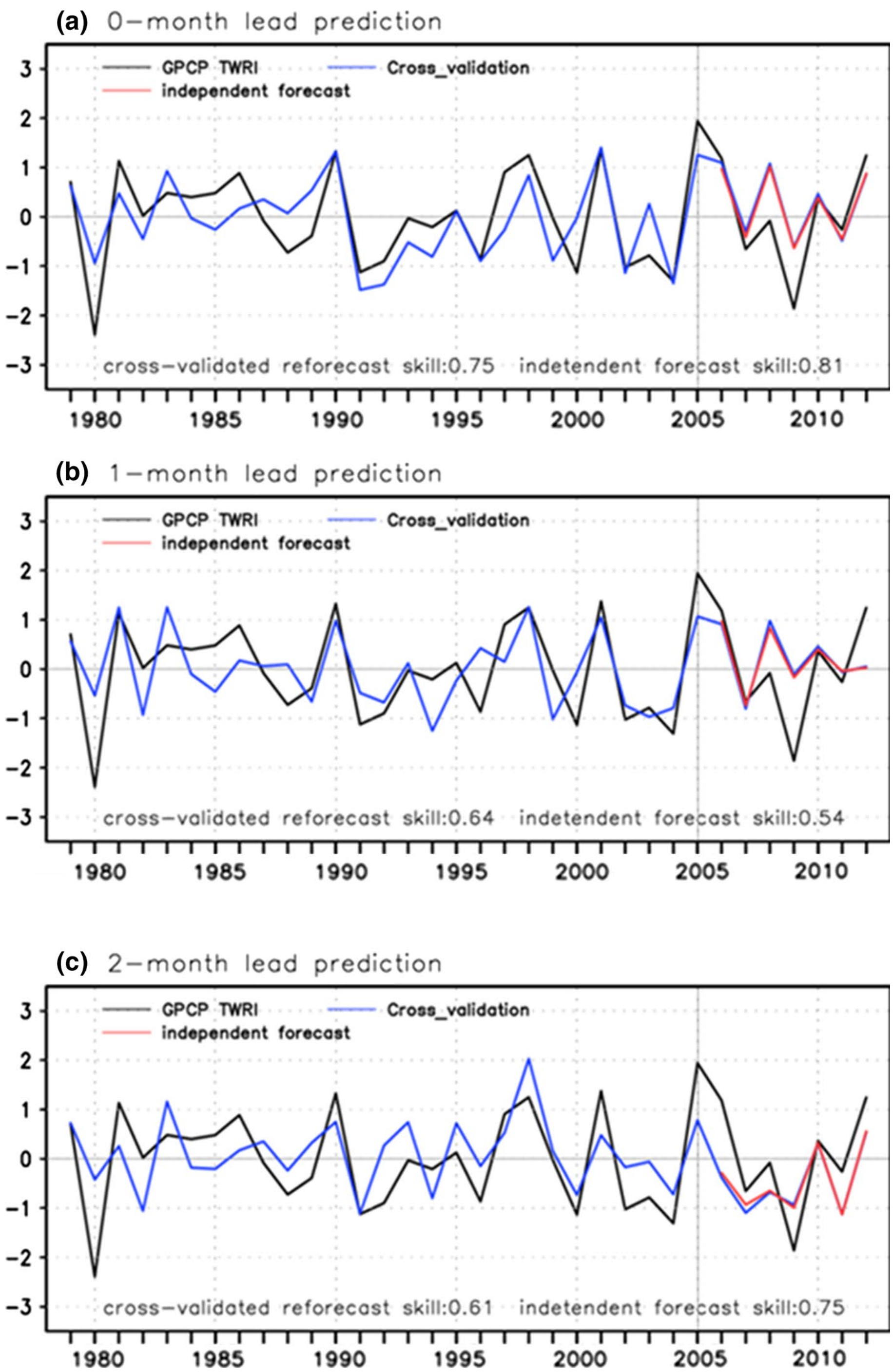

Fig. 6 Prediction skill for the physical–empirical prediction shown by the time series of observation (*black*) and cross-validated predictions by using three predictors of each of **a** 0-month, **b** 1-month, and **c** 2-month lead (*blue*) for the period 1979–2012 (34-year). The cross validation was done by taking 3-year out around the predicted year. The cross-validated correlation skill is 0.75, 0.64, and 0.61 for 1979–2012 at the 0-, 1-, and 2-month lead time, respectively. The 2006–2012 values (*red*) are independent test predictions when the model is built using the data in the training period of 1979–2005

Table 3 Same as Table 2 except for 1-month lead

	TWRI	IOWPT	NAT	EAT
TWRI	1.0	**0.50**	**0.48**	**0.43**
IOWPT	–	1.0	0.18	0.14
NAT	–	–	1.0	0.13
EAT	–	–	–	1.0

Table 4 Same as Table 2 except for 2-month lead

	TWRI	IOWPT	NAT	EAT
TWRI	1.0	**0.52**	**0.54**	0.31
IOWPT	–	1.0	0.27	0.10
NAT	–	–	1.0	0.31
EAT	–	–	–	1.0

to steep topography that hardly hold rain water. Meiyu is the first intensive rainy period after the dry season from October to April. Prediction of Meiyu onset and rainfall amount is of critical importance to water resource management. There is a high demand for rainfall prediction from sub-seasonal to seasonal scales. Yet the state-of-the-art dynamical models' multi-model ensemble prediction has limited skill, the temporal correlation skill for hindcast of MJ precipitation in the rectangular region around Taiwan (119E–123E and 21N–26N) is only 0.37 during 1979–2010 (Fig. 2b).

In order to predict Taiwan Meiyu rainfall, we have identified three physical consequential precursors (Fig. 5). The first precursor is a dipolar SST anomaly tendency in the Indo-Pacific warm pool (IOWPT), which signifies development of Philippine Sea anomalous anticyclone that can maintain itself until early summer through anticyclone-SST dipole interaction (Wang et al. 2000; Lau et al. 2005). The second predictor is a tripolar SST anomaly tendency over North Atlantic (NAT), which is coupled with North Atlantic Oscillation (NAO) and maintains themselves through spring and into MJ (Wu et al. 2009). The third predictor is the warming tendency over the North Asia and East Asia (EAT). The EA continental warming tendency is arguably important for setting up the low pressure anomaly in southeast China in MJ, which enhance the EA subtropical frontal zone.

A suite of prediction models were built using the three predictors to make prediction of MJ Taiwan Meiyu with 0-, 1-, and 2-month lead, respectively. These predictors essentially represent the same three different physical processes, indicating the robustness of the predictors. The cross-validated correlation skill for Taiwan Meiyu forecast is significantly higher than the dynamical models' hindcast, suggesting that (1) the physical–empirical model can be a useful complementary tool for seasonal prediction, and (2) there is a large room for improvement of the current climate models. In particular, it can be fruitful to examine how the models capture the processes discussed earlier in this paper.

The Taiwan Meiyu season is associated with the large-scale East Asia (EA) subtropical rain band located to the northwest flank of the western North Pacific subtropical high (WNPSH) (Fig. 2a). Thus, the Taiwan Meiyu rainfall index (TWRI) reflects not only the 24 stations at Taiwan (Fig. 3) but also the EA subtropical monsoon variability in early summer. The MJ Taiwan rainfall anomaly is strongly connected to positive rainfall variability over southeast China ($r = 0.75$). Since the Taiwan Meiyu represent the large scale rainfall variability over the EA subtropical front (Fig. 2a), these physical predictors can potentially be used for rainfall prediction along the EA subtropical front in early summer and the anomalies over the South China, Southeast Asia and East Asia.

The physical processes discussed in this paper may be useful for further development of dynamic-empirical prediction models which utilize the climate model's output to make a "downscaling" forecast of the local rainfall anomalies. In addition, we plan to use Taiwan Meiyu index for an extended period (1950–2012) or long-term data to examine whether there exist secular change in predictor–predictand relationship and improve the physical–empirical model proposed in this study.

Acknowledgments This work was jointly supported by APEC climate center (APCC), the National Research Foundation (NRF) of Korea through a Global Research Laboratory (GRL) grant of the Korean Ministry of Education, Science and Technology (MEST, #2011-0021927), and the Central Weather Bureau under the Hazardous Weather Monitoring and Forecasting Systems Enhancement Project. We also acknowledge support from the International Pacific Research Center (IPRC). This is publication No. 9200 of the SOEST, publication No. 1078 of IPRC and publication No. 13 of Earth System Modeling Center (ESMC).

References

Boyle JS, Chen TJ (1987) Synoptic aspects of the wintertime East Asian monsoon. In: Chang CP, Krishnamurti TN (eds) Monsoon meteorology. Oxford University Press, Oxford, pp 125–160

Chen GTJ (1983) Observational aspects of the Meiyu phenomena in subtropical China. J Meteorol Soc Jpn 61:306–312

Chen TC, Yen MC, Hsieh JC, Arritt RW (1999) Diurnal and seasonal variations of the rainfall measured by the automatic rainfall and meteorological telemetry system in Taiwan. Bull Am Meteorol Soc 80:2299–2312

Chen CS, Chen WC, Tao WK (2004) Characteristics of heavy summer rainfall in southwestern Taiwan in relation to orographic effects. J Meteorol Soc Jpn 82:1521–1543

Chen CS, Chen YL, Liu CL, Lin PL, Chen WC (2007) Statistics of heavy rainfall occurrences in Taiwan. Weather Forecast 22:981–1002

Chen JM, Li T, Shih CF (2010) Tropical cyclone-and monsoon-induced rainfall variability in Taiwan. J Clim 23:4107–4120

Dee DP et al (2011) The ERA-interim reanalysis: configuration and performance of the data assimilation system. Q J R Meteorol Soc 137:553–597

Delworth TL, Broccoli AJ, Rosati A et al (2006) GFDL's CM2 global coupled climate models. Part I: formulation and simulation characteristics. J Clim 19:643–674

Gong DY, Yang J, Kim SJ, Gao Y, Guo D, Zhou T, Hu M (2011) Spring Arctic Oscillation-East Asian summer monsoon connection through circulation changes over the western North Pacific. Clim Dyn 37:2199–2216

Hudson D, Alves O, Hendon HH, Wang G (2011) The impact of atmospheric initialisation on seasonal prediction of tropical Pacific SST. Clim Dyn 36:1155–1171

Huffman GJ, Bolvin DT, Adler RF (2011) Last updated GPCP Version 2.2 combined precipitation data set. WDC-A, NCDC, Asheville, NC (2011). Dataset accessed at http://www.ncdc.noaa.gov/oa/wmo/wdcamet-ncdc.html

Lau NC, Nath MJ (2003) Atmosphere-ocean variations in the Indo-Pacific sector during ENSO episodes. J Clim 16:3–20

Lau NC, Leetmaa A, Nath MJ, Wang HL (2005) Influences of ENSO-induced Indo-western Pacific SST anomalies on extratropical atmospheric variability during the boreal summer. J Clim 18:2922–2942

Luo JJ, Masson S, Behera S, Shingu S, Yamagata T (2005) Seasonal climate predictability in a coupled OAGCM using a different approach for ensemble forecast. J Clim 18:4474–4497

Panofsky HA, Brier GW (1968) Some applications of statistics to meteorology. Pennsylvania State University Press, Pennsylvania

Saha S, Nadiga S, Thiaw C et al (2014) The NCEP climate forecast system version 2. J Clim 27:2185–2208

Smith TM, Reynolds RW, Peterson TC, Lawrimore J (2008) Improvements to NOAA's historical merged land-ocean surface temperature analysis (1880–2006). J Clim 21:2283–2296

Tao S, Chen LX (1987) A review of recent research on the East Asian summer monsoon in China. In: Chang C-P, Krishnamurti TN (eds) Monsoon meteorology. Oxford University Press, Oxford, pp 60–92

Wang B, LinHo (2002) Rainy seasons of the Asian-Pacific monsoon. J Clim 15:386–398

Wang ST, Cheng H, Chao YK (1984) Natural seasons of the weather in the Taiwan area. Atmos Sci (Taiwan) 11:101–120

Wang B, Wu R, Fu X (2000) Pacific-East Asia teleconnection: how does ENSO affect East Asian climate? J Clim 13:1517–1536

Wang B, Lee JY et al (2009a) Advance and prospectus of seasonal prediction: assessment of the APCC/CliPAS 14-model ensemble retroperspective seasonal prediction (1980–2004). Clim Dyn 33:93–117

Wang B, Liu J, Yang J, Zhou T, Wu Z (2009b) Distinct principal modes of early and late summer rainfall anomalies in East Asia. J Clim 22:3864–3875

Wang B, Xiang B, Lee JY (2013) Subtropical high predictability establishes a promising way for monsoon and tropical storm predictions. PNAS 10:2718–2722

Wu Z, Wang B, Li J, Jin FF (2009) An empirical seasonal prediction of the East Asian summer monsoon using ENSO and NAO. J Geophys Res 114:D18120. doi:10.1029/2009JD011733

Yen MC, Chen TC (2000) Seasonal variation of the rainfall over Taiwan. Int J Climatol 20:803–809

Yim SY, Jhun JG, Lu R, Wang B (2010) Two distinct patterns of spring Eurasian snow cover anomaly and their impacts on the East Asian summer monsoon. J Geophys Res 115:D22113. doi:10.1029/2010JD013996

Yim SY, Wang B, Kwon M (2013) Interdecadal change of the controlling mechanisms for East Asian early summer rainfall variation around the mid-1990s. Clim Dyn 42:1325–1333